Lattice Boltzmann Simulation for the Optimized Surface Pattern in a Micro-Channel *

WANG Jin-Feng(王金凤)[1,2], LIU Yang(刘扬)[2**], XU You-Sheng(许友生)[1,2***], WU Feng-Min(吴锋民)[1]

[1]*Department of Physics, Zhejiang Normal University, Jinhua 321004*

[2]*Department of Mechanical Engineering, The Hong Kong Polytechnic University, Hong Kong*

(Received 15 March 2007)

Based on the Bhatangar–Gross–Krook (BGK) models, numerical simulation using the lattice Boltzmann model is performed to investigate the optimized surface pattern in a micro-channel. In order to simulate the practical situation correctly, a slip/no-slip boundary condition is applied with making several assumptions. To assess the validity and efficiency of the model, one benchmark problem with considering the surface patterns is studied. Numerical results show the value of rms velocity $V_{\rm rms}$ increases with the increasing ratio β and larger Reynolds number Re, higher fluctuation of the rms oscillating velocity. Furthermore, the results show that a good mixing effect can be obtained when Re is large enough and the ratio β is about 1.618, which is the appropriate choice, i.e. the well known golden section phenomenon.

PACS: 47. 55. Mh, 03. 40. Kf, 02. 70. − c

Flow in a micro-channel is the term used to describe flow in devices with dimensions ranging from millimetres to micrometres which is capable of handling volumes of fluid in the range of nanometres to micrometres. In the last few years there has been an explosion of works in this area due to promising potential applications in micro-fluidics, especially in micro electrical mechanical systems (MEMS). As may be expected, there is now a considerable amount of literature on various aspects of micro-fluidics spreading over many sub-areas: micro fabrication techniques, new designs, interface with MEMS technologies, basic fluid mechanical aspects, etc.[1−7]

To our knowledge, flows in micro-channel are usually treated by volume average approaches. Due to the fact that its boundaries and structures are complicated, the lattice gas automata and lattice Boltzmann methods (LBMs) are often used to treat these problems. One of the earliest studies, reported in Ref. [8], concerned with the validity of Darcy's law for a 2D system constructed by randomly placed solid points. In this Letter, an LBM is applied to simulate the optimized surface pattern in a micro-channel.

We can start from the following kinetic equation:

$$n_i(\boldsymbol{x}+\boldsymbol{\xi}_i\delta t, t+\delta t) = n_i(\boldsymbol{x}, t) + \delta_i, \tag{1}$$

where δ_i is the collision function of the model. The Boltzmann equation can be written as

$$\frac{\partial f}{\partial t} + \boldsymbol{\xi}\Delta f = J(f), \tag{2}$$

where $\boldsymbol{\xi}$ is the particle velocity, f is the Maxwellian distribution function, $J(f)$ is the collision operator. Equation (2) can be derived from expansion of the left term of Eq. (1). We have

$$n_i(x+\boldsymbol{\xi}_i\delta t, t+\delta t) = n_i(x,t) + \delta t\frac{\partial n_i}{\partial t} + \boldsymbol{\xi}_i\delta t\nabla n_i + O((\delta t)^2). \tag{3}$$

Neglecting the higher order terms, one obtains

$$\frac{\partial n_i}{\partial t} + \boldsymbol{\xi}_i\nabla n_i = \frac{\delta_i}{\delta t}. \tag{4}$$

Substituting $n_i \to f$, $\boldsymbol{\xi}_i \to \boldsymbol{\xi}$, $\delta_i/\delta t \to J(f)$ gives the Boltzmann Eq. (2). Based on the BGK approximation, the Boltzmann equation reads

$$\frac{\partial f}{\partial t} + \boldsymbol{\xi}\nabla f = -\frac{1}{\tau}(f - f^{(eq)}). \tag{5}$$

By Taylor series expansion, Eq. (2) reduces to

$$f(\boldsymbol{x}+\boldsymbol{\xi}\delta t, \boldsymbol{\xi}, t+\delta t) - f(\boldsymbol{x}, \boldsymbol{\xi}, t) = -\frac{1}{\tau}[f(\boldsymbol{x}, \boldsymbol{\xi}, t) - f^{(eq)}(\boldsymbol{x}, \boldsymbol{\xi}, t)], \tag{6}$$

where τ and δt are the relaxation time and discretized time interval, respectively.

Further distribution in phase space, following the appropriate approximation of the equilibrium distribution and low Mach number assumption leads to the single time relaxation-lattice Boltzmann equation (SRT-LBE) in the form

$$f_i(\boldsymbol{x}+\boldsymbol{e}_i\delta t, t+\delta t) - f_i(\boldsymbol{x}, \boldsymbol{e}_i, t) = -\frac{1}{\tau}[f_i(\boldsymbol{x}, \boldsymbol{e}_i, t) - f_i^{(eq)}(\boldsymbol{x}, \boldsymbol{e}_i, t)], \quad i = 0-k, \tag{7}$$

where $f_i^{(eq)}$ is the discretized equilibrium distribution function and $\boldsymbol{e}_i$ is the discrete velocity set, both based

* Supported by the National Natural Science Foundation of China under Grant No 10572130, the Research Grants Council of the Government of the HKSAR under Grant No PolyU5231/06E, the National Basic Research Programs of China under grant 2006CB708612.

** Email: mmyliu@polyu.edu.hk

*** Email: Ysyou@zjnu.cn

©2007 Chinese Physical Society and IOP Publishing Ltd

on the lattice model. For the D_2Q_9 model, $\boldsymbol{e}_i$ is given by (as shown in Fig. 1)

$$\boldsymbol{e}_i = \begin{cases} 0, & (i=0) \\ \left[\cos\left(\frac{(i-1)\pi}{2}\right), \sin\left(\frac{(i-1)\pi}{2}\right)\right]c, & (i=1-4) \\ \left[\cos\left(\frac{\pi}{4}+\frac{(i-5)\pi}{2}\right), \right. \\ \quad \left. \sin\left(\frac{\pi}{4}+\frac{(i-5)\pi}{2}\right)\right]\sqrt{2}c, & (i=5-8) \end{cases} \tag{8}$$

where c, δx and δt are the particle streaming speed, lattice constant and time step, respectively.

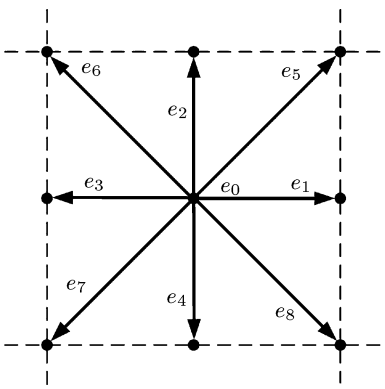


Fig. 1. Discrete velocity vector for the D_2Q_9 lattice.

According to Refs. [9–11], this velocity is related to the thermal velocity of the fluid particles and determined by the fluid temperature T, the Boltzmann constant R and the mass m of the particles read

$$c = \sqrt{3}c_s = \sqrt{\frac{3RT}{m}}, \tag{9}$$

where c_s is the speed of sound with $c_s = 1/3$. We take the kinetic viscosity $v = (2\tau - 1)\delta t/6$. The fluid density ρ and the fluid velocity $\boldsymbol{u}$ are defined by

$$\rho = \sum_{i=0}^{k} f_i = \sum_{i=0}^{k} f_i^{eq},$$
$$\rho\boldsymbol{u} = \sum_{i=0}^{k} f_i\boldsymbol{e}_i = \sum_{i=0}^{k} f_i^{eq}\boldsymbol{e}_i. \tag{10}$$

An isolated system, after a long period of time, should reach an equilibrium state.[12,13] Considering the H function

$$H(\boldsymbol{x}, t) = \int f \ln f d\boldsymbol{\xi}, \tag{11}$$

differentiating Eq. (11) with respect to time one obtains

$$\frac{\partial H}{\partial t} = \int (1 + \ln f)\frac{\partial f}{\partial t} d\boldsymbol{\xi}. \tag{12}$$

If we only consider a spatially uniform system, i.e., f depends on t, Eq. (12) can be written as

$$\frac{\partial H}{\partial t} = \int (1 + \ln f) J(f) d\xi. \tag{13}$$

Then the collision function $J(f)$ can be written as[12]

$$J(f) = \frac{1}{m} dS d\boldsymbol{\xi}_1 |\boldsymbol{\xi}_1 - \boldsymbol{\xi}| (f' f_1' - f f_1), \tag{14}$$

where dS is the collision cross section; f_1, f_1', f and f' are defined as $f_1 \equiv f(\boldsymbol{x}, \boldsymbol{\xi}_1, t)$, $f_1' \equiv f(\boldsymbol{x}, \boldsymbol{\xi}_1', t)$, $f' \equiv f(\boldsymbol{x}, \boldsymbol{\xi}', t)$ and $f \equiv f(\boldsymbol{x}, \boldsymbol{\xi}, t)$, respectively; $\boldsymbol{\xi}'$ and $\boldsymbol{\xi}_1'$ are the molecular velocities before a binary collision. Based the momentum and energy conservation laws, Eq. (14) can be rewritten as

$$\frac{\partial H}{\partial t} = \frac{1}{4m} \int dS d\boldsymbol{\xi} d\boldsymbol{\xi}_1 |\boldsymbol{\xi}_1 - \boldsymbol{\xi}| (f' f_1' - f f_1) \ln \frac{f f_1}{f' f_1'}, \tag{15}$$

as $(f' f_1' - f f_1) \ln(f f_1 / f' f_1') \leq 0$, we can obtain

$$\frac{\partial H}{\partial t} \leq 0. \tag{16}$$

Equation (16) means that the H function can never increase with time. Indeed, it is the Boltzmann's H-theorem. When $f' f_1' = f f_1$, Eq. (16) will relate to the equilibrium state. Then the condition can be expressed as

$$\ln f + \ln f_1 = \ln f' + \ln f_1'. \tag{17}$$

The above description of the equilibrium state indicates that $\ln f$ in this state is a collision invariant, so that

$$\ln f^{(eq)}(\boldsymbol{\xi}) = A + \boldsymbol{B} \cdot \boldsymbol{\xi} + C\boldsymbol{\xi}^2, \tag{18}$$

where the constants A, $\boldsymbol{B}$ and C are not arbitrary. We can substitute Eq. (18) for the following equations including mass density equation, momentum equation, and energy density equation,

$$\rho(\boldsymbol{x}, t) = \int f(\boldsymbol{x}, \boldsymbol{\xi}, t) d\boldsymbol{\xi}, \tag{19}$$

$$\rho\boldsymbol{u}(\boldsymbol{x}, t) = \int \boldsymbol{\xi} f(\boldsymbol{x}, \boldsymbol{\xi}, t) d\boldsymbol{\xi}, \tag{20}$$

$$\rho e(\boldsymbol{x}, t) = \frac{1}{2} \int \boldsymbol{\xi}_0^2 f(\boldsymbol{x}, \boldsymbol{\xi}, t) d\boldsymbol{\xi}. \tag{21}$$

We can obtain the unique equilibrium distribution function as

$$f^{(eq)}(\boldsymbol{\xi}) = \frac{\rho}{(2\pi RT)^{3/2}} \exp\left[\frac{-m(\boldsymbol{\xi} - \boldsymbol{u})^2}{2RT}\right]. \tag{22}$$

For the D_2Q_9 model, the equilibrium distribution function can be chosen in the form

$$f_i^{(eq)} = t_i \rho [1 + 3(\boldsymbol{e}_i \cdot \boldsymbol{u}) + 4.5(\boldsymbol{e}_i \cdot \boldsymbol{u})^2 - 1.5\boldsymbol{u} \cdot \boldsymbol{u}], \quad i = 0-8, \tag{23}$$

with

$$t_0 = \frac{4}{9}, t_{1,2,3,4} = \frac{1}{9}, \ t_{5,6,7,8} = \frac{1}{36}. \tag{24}$$

As a primary method in the lattice Boltzmann simulation, bouncing-back boundary condition has been proven to possess the first-order accuracy.[14] More accurate boundary conditions have been proposed in the past few years.[15–19] In this study, the pressure boundary condition is implemented. As we know,

pressure is related to the density by the isothermal equation of state as $p = c_s\rho$ (c_s is the sound speed). Specification of the pressure on a flow boundary is proposed as shown in Fig. 2. Suppose a flow boundary is along the y-direction, and the pressure is specified. Take the inlet in Fig. 2 for example, u_y is supposed to be specified too. After streaming, f_2, f_3, f_4, f_6, f_7 are known, $\rho = \rho_{in}$, $u_y = 0$ are specified at the inlet. We can obtain u_x and f_1, f_5, f_8 from Eq. (10):

$$\begin{aligned}
&\rho_{in} = f_0 + f_1 + f_2 + f_3 + f_4 + f_5 + f_6 + f_7 + f_8,\\
&\rho_{in}u_x = f_1 - f_3 + f_5 - f_7 + f_8 - f_6,\\
&\rho_{in}u_y = f_2 - f_4 + f_5 - f_7 + f_6 - f_8.
\end{aligned} \tag{25}$$

Consistency of Eq. (25) gives

$$u_x = \frac{(\rho_{in} - (f_0 + f_2 + f_4 + 2(f_3 + f_6 + f_7)))}{\rho_{in}}. \tag{26}$$

At the inlet, using the non-equilibrium part of the particle distribution, we can find $f_1 - f_1^{(eq)} = f_3 - f_3^{(eq)}$. When f_1 is known, f_5 and f_8 are obtained from Eq. (25),

$$\begin{aligned}
f_1 &= f_3 + \frac{2}{3}\rho_{in}u_x,\\
f_5 &= f_7 - \frac{1}{2}(f_2 - f_4) + \frac{1}{6}\rho_{in}u_x,\\
f_8 &= f_6 + \frac{1}{2}(f_2 - f_4) + \frac{1}{6}\rho_{in}u_x.
\end{aligned} \tag{27}$$

The corner node at the inlet or outlet needs some special treatment. Take the bottom node at the inlet for example, after streaming, f_3, f_4, and f_7 are known. Here ρ is specified, and $u_x = u_y = 0$. We need to determine f_1, f_2, f_5, f_6, f_8 and use the non-equilibrium part of the particle distribution normal to the inlet and the boundary to find

$$\begin{cases} f_1 - f_1^{(eq)} = f_3 - f_e^{(eq)} \\ f_2 - f_2^{(eq)} = f_4 - f_4^{(eq)} \end{cases} \Rightarrow \begin{cases} f_1 = f_3, \\ f_2 = f_4. \end{cases} \tag{28}$$

Using f_1 and f_2 in Eq. (25), we can find

$$\begin{aligned}
&f_5 = f_7,\\
&f_6 = f_8 = \frac{1}{2}[\rho_{in} - (f_0 + f_1 + f_2 + f_3 + f_4 + f_5 + f_7)].
\end{aligned} \tag{29}$$

A similar procedure can be applied to top inlet nodes and outlet nodes including outlet corner nodes. The case of ρ and non-zero u_y at a flow boundary along the y-direction can be handled in the same way.

For a long time, researchers have applied the no-slip boundary condition to fluid flow over a solid surface. Navier[20] proposed the possibility of fluid slip. He assumed that the velocity u_x at a solid surface is proportional to the shear rate at the surface,

$$u_x = \chi\frac{du_x}{dy}, \tag{30}$$

where χ is the slip length or slip coefficient. If $\chi = 0$, the boundary condition is assumed to be no-slip. If χ is finite, fluid slip occurs at the wall, while its effect depends upon the length scale on the flow. In this work, the bounce back boundary condition at the top and bottom walls, respectively, follows

$$\begin{cases} f_4(i,N,t) = f_2(i,N-1,t), \\ f_7(i+1,N,t) = f_5(i,N-1,t), \\ f_8(i-1,N,t) = f_6(i,N-1,t); \end{cases}$$
$$\begin{cases} f_2(i,0,t) = f_4(i,1,t), \\ f_5(i-1,0,t) = f_7(i,1,t), \\ f_6(i+1,0,t) = f_8(i,1,t). \end{cases} \tag{31}$$

The specular reflection boundary conditions at the top and bottom walls are, respectively,

$$\begin{cases} f_4(i,N,t) = f_2(i,N-1,t), \\ f_8(i-1,N,t) = f_5(i-1,N-1,t); \\ f_7(i+1,N,t) = f_6(i+1,N-1,t), \end{cases}$$
$$\begin{cases} f_2(i,0,t) = f_4(i,1,t), \\ f_5(i-1,0,t) = f_8(i-1,1,t), \\ f_6(i+1,0,t) = f_7(i+1,1,t). \end{cases} \tag{32}$$

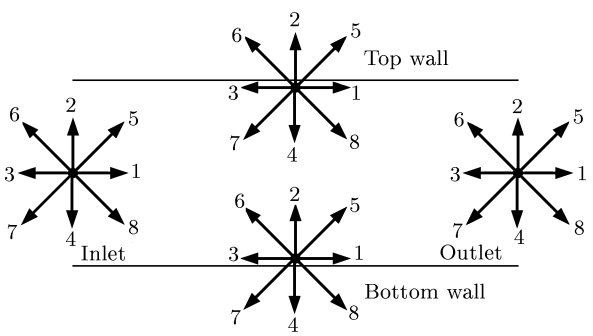


Fig. 2. Display of distribution functions at boundary points.

In this work, Kn is less then 0.01, and no-slip and slip boundary conditions are used at hydrophobic and hydrophilic surfaces, respectively. Figure 3 shows the surface patterns of the case considered. Here we address the question of pressure-driven flow in a microchannel that is patterned with alternating region of no-slip and perfect slip boundary conditions. They take the form of rings of hydrophilic region transverse to hydrophobic region and are distributed periodically along the channel with a period $0.5 + 0.5\beta$. Here β, named slip/no-slip, is defined as the ratio of the hydrophobic width to the hydrophilic width.

Firstly, we simulate the value of rms velocity $V_{\rm rms}$ for the y-direction when β is equal to 10/30, 10/25, 10/20, 10/19, 10/18, 10/17, 10/16, 10/15, 10/14, 10/13, 10/12, 1, 12/10, 13/10, 14/10, 15/10, 16/10, 17/10, 18/10, 19/10, 20/10, 25/10, 30/10 for different Reynolds numbers. Figure 4 shows the variation of rms oscillating velocity with the different ratio β and the different Re. Figure 5 shows the variation of rms oscillating velocity along the middle line for the different ratio β and different Re. It can be found from

Figs. 4 and 5 that $V_{\rm rms}$ increases with the increasing ratio β. However, after the ratio β achieves a definite value, $V_{\rm rms}$ starts to reduce. From Figs. 4 and 5 it is seen that the highest rms oscillating velocity occurs at the point with the ratio β of about 1.6. Meanwhile, comparing rms oscillating velocities under the different Re, we can find that the rms velocity increases with the increasing Re.

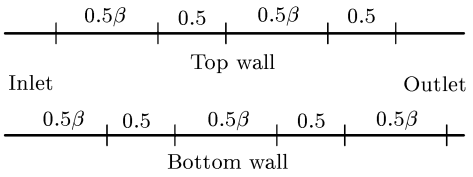


Fig. 3. Alternative surface pattern, i.e., the hydrophobic and the hydrophilic sections arranged alternatively between the top and bottom walls.

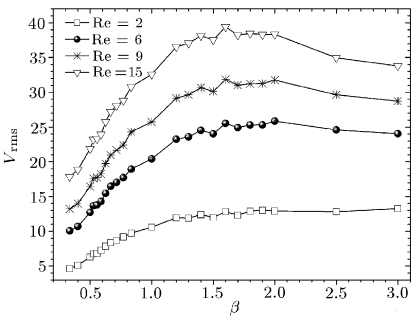


Fig. 4. The rms value of all oscillating velocities for different β and Re.

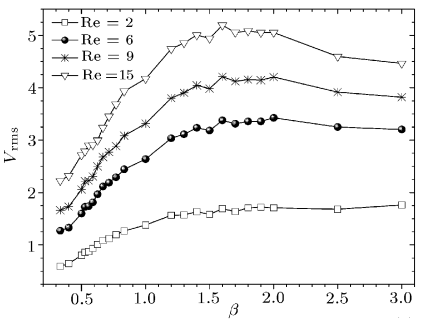


Fig. 5. The rms oscillating velocity along the middle line for different β and Re.

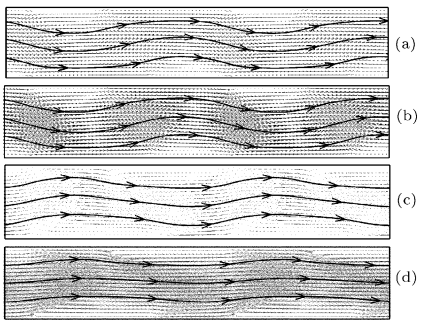


Fig. 6. Oscillating flow patterns for alternative surface patterns (a) at $Re = 2$, (b) $Re = 9$, (c) $Re = 20$, (d) $Re = 80$.

Figure 6 shows the oscillating flow patterns for different Reynolds numbers. They separately express the fluid flow phenomenon in the identical region with the same ratio β of 1.6. The grey arrows indicate the direction of the flow. Figure 7 shows the flow patterns with no alternative surface pattern. In face, the fluid is a Poiseuille flow. From Figs. 6 and 7, it is obvious that the introduction of the alternative surface pattern in the micro-channel yields the flow oscillation. Moreover, Figs. 4 and 5 also explain the flow oscillation. The larger the value of $V_{\rm rms}$, the more intense the fluid oscillation.

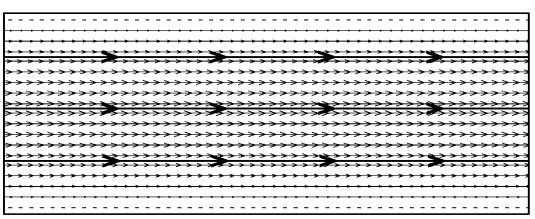


Fig. 7. Numerical results of the flow in a micro-channel with single hydrophilic surface at $Re = 20$.

In comparison of the above analogue results, it is found that the oscillating effect is best when the ratio β is about 1.6. The appropriate choice of the ration is very close to 1.618 that is a golden section of a surface. It is a much interesting phenomenon and all the simulating results support such conclusion.

References

[1] Sun X M, He F and Ding Y T 2003 *Chin. Phys. Lett.* **20** 2199

[2] Xu Y S, Liu Y and Huang G X 2004 *Chin. Phys. Lett.* **21** 2454

[3] Xu Y S and Wu F M 2002 *Chin. Phys. Lett.* **19** 1835

[4] Mayeed M S, Mian A, Auner G W and Newaz G M 2006 *J. Biomech. Eng.* **128** 458

[5] Hetsroni G, Mosyak A, Pogrebnyak E and Yarin L P 2005 *Int. J. Heat Mass Transfer.* **48** 1982

[6] Gravesen P, Branebjerg J and Jensen O S 1993 *J. Micromech. Microeng.* **3** 168

[7] Chen H Y and Lahann J 2005 *Ann. Chem.* **77** 9609

[8] Chu K H W 2002 *Eur. J. Appl. Phys.* **17** 131

[9] He X and Luo L S 1997 *Phys Rev.* E **55** 479

[10] He X and Luo L S 1970 *Phys Rev.* E **56** 6188

[11] Luo L S 2000 *Phys. Rev.* E **62** 4982

[12] Luo L S, 1993 *PhD Dissertation* (Georgia Institute of Technology)

[13] Barrat J and Bocquet L 1999 *Phys. Rev. Lett.* **82** 4671

[14] Noble D R, Chen S, Georgiadis J G and Buckius R O 1995 *Phys. Fluids* **7** 203

[15] Fang H P, Lin Z F and Wang Z W 1998 *Phys. Rev.* E **57** R25

[16] He X, Zou Q and Dembo M 1997 *J. Stat. Phys.* **87** 115

[17] Filippova Q and Hanel D 1997 *Comput. Fluids* **26** 697

[18] Guo Z L, Zheng C G and Shi B C 2002 *Phys. Fluids* **14** 2007

[19] Mei R W, Luo L S and Shyy W 1999 *J. Comput. Phys.* **155** 307

[20] Navier C L 1823 *Memoirs de 1'Academie Royale des Sciences de 1'Institute de France* **1** 414